Alpha-Particle Activity of Apollo 11 Samples

Abstract. *Nine polished thin sections have been exposed to nuclear track plates, three have been counted by alpha-particle spectrometry, and one has been examined by electron microprobe. Interpretation of the results is in a preliminary stage. Alpha track distribution in the autoradiograph of a breccia forms a network that appears related to the rims of accretionary lapilli composing the breccia. Thorium in a coarse-grained crystalline rock is concentrated in micron-sized, zirconium-rich crystals. Alpha count rates agree with what would be predicted from previously reported thorium and uranium contents of the same rocks, suggesting secular equilibrium for the thorium and uranium decay series.*

Polished, uncovered thin sections of Apollo 11 samples were studied by α-particle autoradiography, α-particle spectrometry, and electron microprobe in an effort to determine the distribution of the α-emitting nuclides, that is, thorium and uranium and their radioactive daughters within the lunar samples. This study was restricted to nondestructive analysis. So far, nine samples have been exposed to nuclear track plates for periods of 2 to 5 weeks. Of these, one track plate has been examined in detail and the others have been scanned in reconnaissance with the petrographic microscope. Alpha-particle spectrometric measurements have been made on three samples. One sample has been analyzed with the electron microprobe.

The autoradiograph of breccia sample number 19,14 has been studied in detail. Figure 1A is a photomicrograph of the sample, and Fig. 1B is a map of the autoradiograph of the sample, showing the distribution of α tracks. Figure 1B shows track density ranging from approximately 300 to 500 tracks per square centimeter for 1 by 1 cm areas. Considering smaller areas, 0.25 by 0.25 cm, the track density varies from approximately 175 to 700 tracks per square centimeter over the area of the sample. This autoradiograph represents a 2-week exposure of the nuclear track plate to the sample.

Groupings of α tracks seen in Fig. 1B indicate areas of thorium or uranium enrichment that are larger than individual rock or crystal fragments, and there appears to be a reticulate pattern to the track distribution. Petrographic examination of the textures of sample 19,14 and other breccias shows that they are composed of ovoid, accretionary lapilli, which have a concentric internal structure. The lapilli generally have a crystal fragment core, surrounded by glass and fine crystal shards and mantled by glass or by glass rimmed by coarse crystal shards. The more prominent lapilli can be seen in Fig. 1A outlined by arcuate chains of crystal fragments. Lapilli range in size from several millimeters to less than 50 μ. Larger lapilli often are composed of aggregates of smaller individually distinguishable lapilli. The matrix between lapilli is the same material which forms the lapilli.

Approximately one third of the breccia is void space, of which we estimate one third is noninterconnected and two thirds are connected. An independent calculation of total void space can be made from the grain density of the fines, 3.1 g/cm^3 (*1*), and the measured bulk densities of 2.0 $\pm$ 0.2 g/cm^3 and 2.02 $\pm$ 0.15 for breccias 18 and 19, respectively (*2*). This calculation indicates that the breccias have 35 percent void space. The bulk densities of the two breccia samples are little more than that of mechanically compacted lunar soil, 1.80 g/cm^3 (*1*), indicating that a minimum of flowage and fracturing is associated with lithification.

Although the breccias contained shocked materials and shock-produced glass, they do not show the textural features characteristic of shock compacted rocks (*3*). The fracture sets, which cut through glass, rock fragments, and matrix without deflection, appear to have formed after induration and probably during excavation of the rock by impact from the original site of deposition. The breccias are bonded together by lightly sintered glass at the

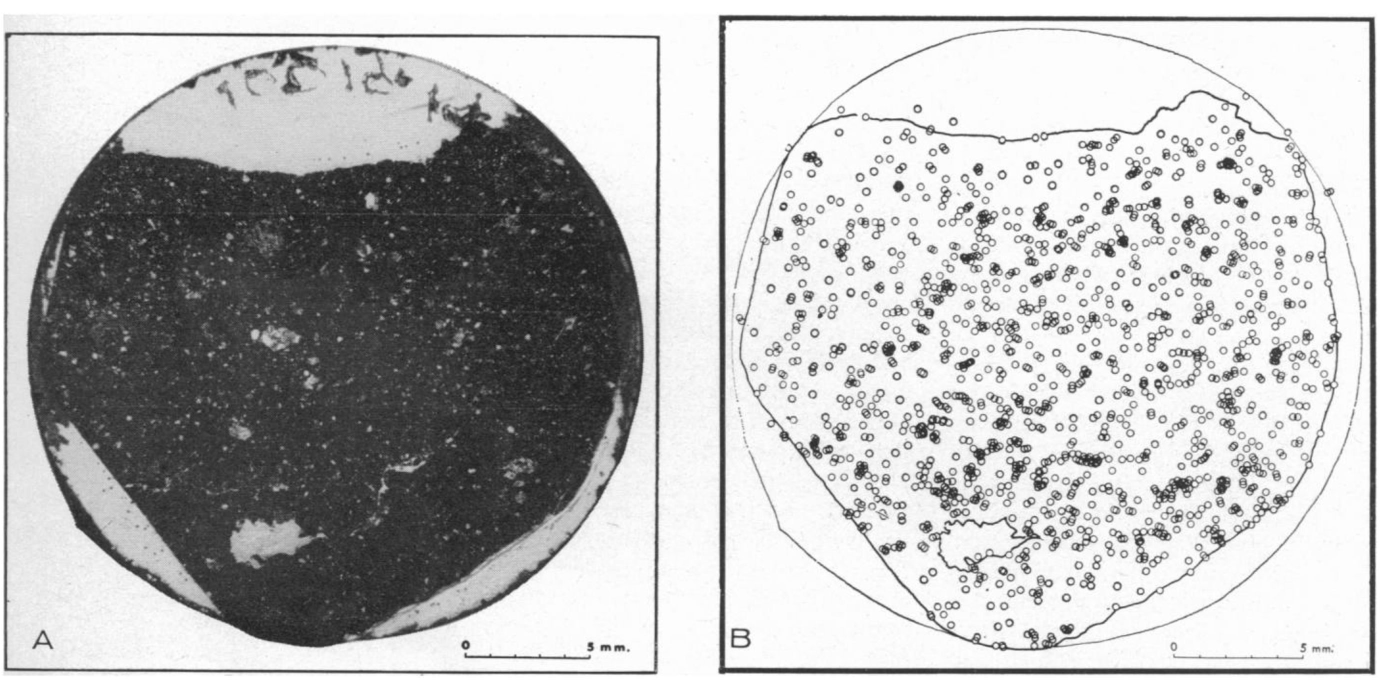

Fig. 1. (A) Photomicrograph of breccia sample 19,14. The breccia is composed of accretionary lapilli, and some of the lapilli can be seen outlined by the arcuate chains of crystal fragments. (B) Map of the autoradiograph of sample 19,14 showing the locations of tracks of α particles.

Table 1. Integral count rates for three lunar samples.

Sample No.	Alpha-particle activity	
	Measured (count hour^{-1}cm^{-2})*	Calculated† (disintegrations hour^{-1}cm^{-2})
17,15	0.50 ± 0.06	4.54
19,14	0.14 ± 0.02	1.94
47,42	0.11 ± 0.06	1.33‡

*Counting efficiency is estimated to be 12 percent. † Based on data from (*1*) and (*2*), assuming secular equilibrium obtains in the thorium and uranium decay series. ‡Based on values for type B rock No. 10003.

points of contact with crystals and other glass. This sintering, most apparent in reflected light photomicrographs, suggests that the temperature of the unit was at or above the softening point for some of the glass fragments. The unit was not hot enough (or thick enough), however, to produce densely welded glass or to cause the glass spherules to flow. Cutler and Hendrichsen (*4*) show that highly angular crushed glass sinters much more rapidly than glass spheres of the same equivalent volume. They show that the rate of sintering is inversely proportional to the radius of glass particles at the point of contact and may be five times faster in angular particles than in spheres. It appears, therefore, that the fine-grained angular lunar glass particles could undergo rapid sintering while the larger or more spherical glass particles and crystalline fragments were relatively unaffected. Rock and crystal fragments would be joined by spot welds produced by sintered, micron-sized glass fragments and sintered angular contacts of larger fragments.

Parts of the network of α tracks shown in Fig. 1A appear to coincide with the outlines of lapilli, which suggests that there is some concentration of radionuclides near the periphery of some of the lapilli.

Scanning of the track plates shows no dense clusters of α tracks. However, numerous, micron-sized, zirconium-rich crystals have been seen in sample 58,46, a course-grained crystalline rock. Figure 2 is a backscattered electron picture of the largest zirconium-rich crystals located in that sample. Microprobe analysis indicates that thorium may be concentrated in this crystal.

We calculate, however, that crystals of the size shown in Fig. 2 would not contain sufficient quantities of thorium or uranium to produce concentrations of α tracks on the nuclear track plates that have been exposed.

Alpha-particle spectrometric measurements have been made on polished sections of samples 17,15 (type A), 19,14 (type C), and 47,42 (type B). The samples, ranging from 220 to 352 mm^2 in area and 30 μ thick were placed 3 mm distant from a 300 mm^2 gold-silicon surface barrier detector. Counts were recorded in a 256-channel spectrum. In this configuration, the total counting efficiency for a similar thick source, 260 mm^2 thorium and uranium-bearing synthetic silicate glass, is 12 percent. The integral count rates for the three lunar samples are given in Table 1, with the calculated number of α-particle decays in the sample. The agreement of the measured α activities with those calculated from reported thorium and uranium values indicates that the thorium and uranium decay series are in equilibrium. The thick-source α-particle spectra accumulated from these samples do not contain sufficient counts to permit spectral analysis.

Our conclusions are as follows.

1) Distribution of α tracks from a breccia section indicates a distribution of the α emitters in the rock related to the texture of the breccia, with the radionuclides concentrated at the periphery of some concretionary lapilli.

2) Electron probe examination of a coarse crystalline rock indicates the presence of numerous micron-sized ziconium-rich crystals which may contain concentrations of thorium.

3) Alpha activity of samples of breccia and crystalline rocks is in agreement with reported thorium and uranium values and indicates secular equilibrium obtains in the thorium and uranium decay series.

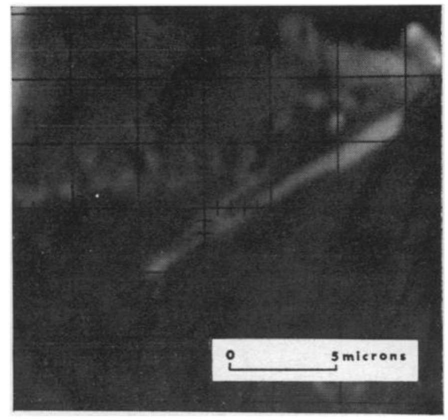

Fig. 2. Backscattered electron picture of zirconium-rich crystal in sample 58,46.

K. A. Richardson, D. S. McKay
W. R. Greenwood, T. H. Foss
Geology Branch, National Aeronautics and Space Administration, Manned Spacecraft Center, Houston, Texas 77058

References

1. Lunar Sample Preliminary Examination Team, *Science* **165**, 1211 (1969).
2. G. D. O'Kelley, J. S. Eldridge, E. Schonfeld, P. R. Bell, personal communication (1969).
3. N. Short, *Science* **154**, 382 (1966).
4. I. B. Cutler and R. E. Henrichsen, *J. Amer. Ceram. Soc.* **51**, 604 (1968).

4 January 1970

Electron-Microprobe Analyses of Phases in Lunar Samples

Abstract. *In fine (type A) and coarse-grained (type B) Apollo 11 lunar volcanic rocks clinopyroxenes are extremely inhomogeneous. Ferrosilite-rich areas in type B rocks have decomposed to submicron vermicular intergrowths of clinopyroxene-fayalite-cristobalite(?). Plagioclase has normal zoning with K_2O up to 0.5 percent in rims. Ilmenites are relatively homogeneous with low MgO (0.1 to 2 percent) and high ZrO_2 (up to 0.26 percent). Metal phase in troilite has <0.02 percent nickel. The breccias (type C) and fines (type D) contain similar phases and aggregates of types A and B together with glassy spherules containing 0.09 to 10.52 percent TiO_2. Rare metal fragments with meteorite-like compositions occur in breccias and fines. Gross similarities between eucrites and Apollo 11 volcanic rocks indicate similar evolutionary environments, but detailed mineralogical differences suggest either separate origins or, if eucrites are lunar, chemical inhomogeneities on the lunar surface.*

In the type A fine-grained volcanic rock studied (10057/67), random microprobe analyses (*1*) of the tiny clinopyroxene grains indicate widely variable Fe (expressed as FeO), Mg, and Ca compositions (Fig. 1). Where larger grains are analyzed the cores are often pigeonitic, whereas the rims are either augite or ferroaugite. Part of the high dispersion apparent in Fig. 1 is due to this zoning of individual grains. One grain analyzed was highly enriched in CaO, with a composition of $Fs_{9.9}$ $En_{1.5}$ $Wo_{88.6}$. The average composition of the clinopyroxene (Table 1) is notable for the appreciable content of Cr_2O_3 and